ELSEVIER

Journal of Nuclear Materials 256 (1998) 218–228

journal of nuclear materials

Effect of oxygen on the operation of a single-cell thermionic fuel element

Dmitry V. Paramonov *, Mohamed S. El-Genk

Institute for Space and Nuclear Power Studies/Chemical and Nuclear Engineering Department, The University of New Mexico, Albuquerque, NM 87131, USA

Received 11 November 1997; accepted 12 March 1998

Abstract

The operation of thermionic converters (TICs) has been shown to be influenced by the presence of tracer amounts of oxygen in the cesium vapor filled interelectrode gap. The induced changes, however, depend on the oxygen and cesium partial pressures and the materials and temperatures of the electrodes. The effects of oxygen on the loss rate from a tungsten emitter surface, by sublimation and formation of volatile tungsten oxides, as a function of oxygen partial pressure were investigated. Results showed that the deposit of the tungsten oxides on the cooler collector affect the converter performance, owing to the induced changes in the collector's oxygenated–cesiated work function and the effective emissivity of the electrodes. Parametric analyses were performed which investigated the effects of introducing tracer amounts of oxygen in the interelectrode gap on the performance parameters of a fission-heated single-cell Thermionic Fuel Element (TFE). These parameters are the electrodes work functions and effective emissivity, the TFE volt–ampere characteristics, the axial distributions of the current density and the electrodes temperatures, and the tungsten loss rate from the emitter surface.

1. Introduction

Thermionic converters (TICs) are being sought for space electric power applications and in topping cycles in terrestrial electric power generation, because they have no moving parts, high reliability and relatively high heat rejection temperature. They operate at typical emitter temperatures of ~1800–1900 K and collector temperatures of 800–1000 K. Because the high temperature in TICs is limited to the emitter, commercial steel and super steel alloys can be used as structural materials for the cooling loop of the collector. Many investigations have attempted to increase the conversion efficiency of TICs, beyond the typical 12–14%, by either increasing the emitter temperature up to 2100 K and/or introducing tracer amounts of oxygen in the cesium vapor filled interelectrode gap (typically $\leqslant 0.5$ mm wide). When operating at such high emitter temperature, however, lifetime issues, such as the gradual loss of the emitter material and the effects on TICs performance of the emitter material deposits on the collector surface should be addressed.

The results of laboratory investigations of TICs with isothermal tungsten emitters have demonstrated that the introduction of a tracer amount of oxygen or cesium oxides in the interelectrode gap could significantly improve the converter performance [1–4]. The measured improvement was attributed to two effects:

(a) An increase in the emitter oxygenated bare work function [3], increasing the emission current due to the low oxygenated–cesiated work function of the emitter. Such a low collector work function not only decreases the optimum cesium pressure, corresponding to the maximum TIC electric power output, but also permits the use of a larger interelectrode gap, therefore, increasing the converter reliability.

* Corresponding author. Present address: Westinghouse Electric Corporation, Science and Technology Center, 1310 Beulah Road, Pittsburgh, PA 15235-5098, USA. Tel.: +1-412 256 1656; fax: +1-412 256 2444; e-mail: paramodv@westinghouse.com.

0022-3115/98/$19.00
PII: S0022-3115(98)00057-9

(b) A decrease of the minimum work function of the collector surface when covered with tungsten oxide deposits from the emitter surface, which increased the load voltage.

In recent laboratory tests [4], conversion efficiencies of 18–22% have been achieved. These tests involved a TIC in which oxygen vapor pressure up to $\sim 8 \times 10^{-6}$ Pa was introduced into the cesium filled interelectrode gap. The emitter temperature was >1800 K, the collector temperature was ~680–800 K, and the cesium pressure in the interelectrode gap was varied from 0.5 Torr (67 Pa) to 1.5 Torr (200 Pa)). The TIC had an emitter made of a Chemical Vapor Deposition (CVD) tungsten coating onto molybdenum and an electropolished molybdenum collector.

The introduction of a large amount of oxygen ($>10^{-6}$ Pa) into the interelectrode gap, however, has been shown to accelerate the emitter material loss rate due to the formation of volatile oxides, which deposit on the relatively cold collector surface, reducing the converter's lifetime and performance. In lifetime tests, the collector became coated with layers composed of emitter material reaction products with the gaseous contaminants in the interelectrode gap, such as oxygen, carbon oxides or water [5,6]. In general, the deposits of the emitter material oxides onto the collector surface affect the performance of TICs or Thermionic Fuel Elements (TFEs) in a number of ways:

(a) lower the cesiated collector work function which increases the load voltage, thus increasing the electric power output and the conversion efficiency;

(b) increase the thermal losses and electrical current leakage when deposited onto spacers and insulator surfaces; lowering the electric power output and conversion efficiency;

(c) cause a short circuit between electrodes, if chipped off, during thermal cycling or vibrations, and bridged the electrodes [7] (this process is more likely as the interelectrode gap size decreases due to swelling of the TFE emitter);

(d) deplete the emission layer on the emitter surface (typically tungsten), which can eventually result in the diffusion of the base material to the surface, hence, reducing the emitter's bare work function and increasing its cesiated work function;

(e) increase the effective emissivity of the electrodes, thus lowering the emitter temperature as well as the emission current and conversion efficiency.

The net contribution of all or some of these effects strongly depends on the TFE design and operation conditions. These include the input thermal power, the interelectrode gap size, type of electrode material, load resistance, cesium pressure and the partial pressures of the gaseous contaminants. Therefore, it is important to investigate the effect of these parameters on both the TFE performance and the emitter material loss rate as a function of the oxygen partial pressure in the interelectrode gap. The results of such an investigation would be useful for the ongoing effort to increase the conversion efficiency and lifetime of TICs for various space and terrestrial electric power applications.

The objectives of this work were to: (a) develop an integrated model of a single-cell TFE to investigate the emitter material loss rate and mass transport in and the performance of the TFE in the presence of oxygen in the interelectrode gap; (b) calculate the emitter material loss rate and the composition of the emitter material oxides deposits onto the collector surface; and (c) investigate the effect of the emitter material oxides deposits onto the collector surface on the TFE performance parameters. These parameters include the volt–ampere characteristics (VACs), conversion efficiency, and the axial distributions of the current density, emitter temperature, and the emitter material loss rate. These results were obtained by coupling an emitter material oxidation and transport model [8] to a two-dimensional thermal and thermionic emission model of a single-cell TFE [9].

2. Calculation procedures

Both nuclear and electrically heated, single-cell TFEs experience a non-uniform axial temperature distributions due to non-uniform heating and end heat losses [8–10]. The non-uniform axial temperature distribution causes the partial pressures of the gaseous contaminants, which may be present in the interelectrode gap, the emitter material loss rate, and the composition of the deposits onto the collector surface, to vary axially along the TFE.

The rate of tungsten loss from the emitter surface and the composition of the tungsten oxides deposits onto the collector surface [8] were calculated as a function of the partial pressures of cesium and oxygen in the interelectrode gap. In the present analysis, the input thermal power, the inlet temperature, coolant mass flow rate and the cesium pressure were used in the input to the TFE thermal model [9] to calculate the axial temperature distributions in the electrodes. These temperature distributions were then used in the TFE thermionic emission model [9] to determine the load current and voltage. The total oxygen inventory in the interelectrode gap and the calculated electrode temperatures were used to determine the partial pressures of cesium and oxygen along the TFE for calculating the emitter material loss rate and the composition of its oxide deposits onto the collector surface [8]. The latter was used to calculate the collector's thermal emissivity and the oxygenated–cesiated work functions of the electrodes, and their values were supplied to the TFE thermal and thermionic emission models [9] to calculate the TFE performance parameters. More details on the description of the

emitter material transport model and of the two-dimensional model of a single-cell TFE can be found elsewhere [8,9]. The following sections detail the methods used to determine the oxygenated–cesiated work functions of the electrodes, and present and discuss the results on the effects of oxygen on the electrodes' emission and radiative properties.

2.1. Emitter work function

In this work, an approach suggested by Rasor [11] for calculating the cesiated emitter work function in the presence of oxygen was used. The sorption of oxygen and cesium onto the emitter surface are assumed to be independent. The oxygen atoms become deeply buried and immobilized in their sorption sites, while the much larger cesium atoms are effectively sorbed onto the surface of a W–O substrate and, hence, are highly mobile [11]. In order to calculate the oxygenated–cesiated work function, the increase in the emitter bare work function due to the presence of oxygen was determined first. Once the bare oxygenated emitter work function was determined as a function of the effective oxygen pressure, the oxygenated–cesiated emitter work function was calculated using the NEDSPHI8 subroutine described in [12]. This subroutine implements the phenomenological model of the sorption of cesium neutrals and ions onto a refractory metal surface [12] to calculate the emitter work function as a function of temperature, cesium pressure, and the value of oxygenated emitter bare work function.

Fig. 1 shows the bare work functions of tungsten surfaces with different crystallographic orientations as a function of the ratio of the surface temperature (T_E) to the saturation temperature (T_{O_2}) of oxygen [12]. Increasing T_{O_2} increases the emitter coverage with oxygen and, hence, increases its oxygenated bare work function. In presence of both cesium and oxygen, however, the saturation oxygen pressure was taken to be equal to the oxygen partial pressure which provides the same sorption flux of oxygen onto the emitter surface. In this case, the effective saturation oxygen pressure was calculated as follows:

$$P_{O_2}^{\text{eff}} = \frac{\sqrt{m_{O_2}}}{2S_{O_2}} \sum \frac{yS_{Cs_xO_y} P_{Cs_xO_y}}{\sqrt{m_{Cs_xO_y}}}, \quad (1)$$

where S is the sticking coefficient (or the ratio of impinging and sorption fluxes of each type of molecules) [14,15], and m is the molecular mass (kg). The effective saturation oxygen pressure ($P_{O_2}^{\text{eff}}$) given by Eq. (1) was related to the saturation oxygen temperature (T_{O_2}) through the rational vapor-pressure equation of Wagner et al. [16]. This temperature was then used with the aid of Fig. 1 to determine the effective oxygenated bare work function of the tungsten emitter, depending on its crystallographic orientation.

The tungsten surface layer of a cylindrical emitter, in the state of the art single-cell TFE, is usually applied by the CVD method, which produces a surface with different crystallographic orientations. Tungsten chloride vapor deposition typically produces an emitter with (1 1 0) and (1 1 2) crystallographic orientation for which the average bare work function is about 4.9 eV [17]. The oxygenated bare work function of such an emitter was determined by interpolation between the curves for the (1 1 0) and (1 1 2) surfaces in Fig. 1, for a bare work function of 4.9 eV. The corresponding values of the oxygenated work function (delineated in Fig. 1) were then used in the NEDSPHI8 subroutine to determine the oxygenated–cesiated work function of the tungsten emitter surface.

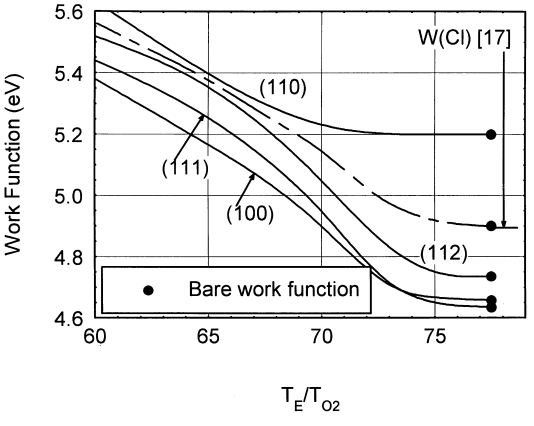

Fig. 1. Tungsten work function data in oxygen vapor [12].

2.2. Collector work function

The cesiated work functions for a pure tungsten collector and for a collector surface covered with tungsten oxide deposits are shown in Fig. 2, as functions of the ratio of the collector temperature (T_C) to the cesium reservoir temperature (T_{Cs}). The minimum work functions for tungsten oxides are lower than for pure tungsten and occur at lower T_C/T_{Cs} ratios, because the low sorption energies of cesium onto tungsten oxides [2]. Bradke and Halder [18] showed that the reduction in the minimum cesiated work function of an oxidized tungsten surface depends on the oxidation conditions, which can be related to the oxygen/tungsten (O/W) ratio of the oxides present on the surface. Because available theoretical models are not valid for calculating the cesiated work function near its minimum [1,11,13], empirical correlations were developed based on the data in the literature for polycrystalline tungsten and tungsten oxides (see Fig. 2). The data in Fig. 2 are for O/W ratio from zero, for a polycrystalline tungsten surface [19,20] to

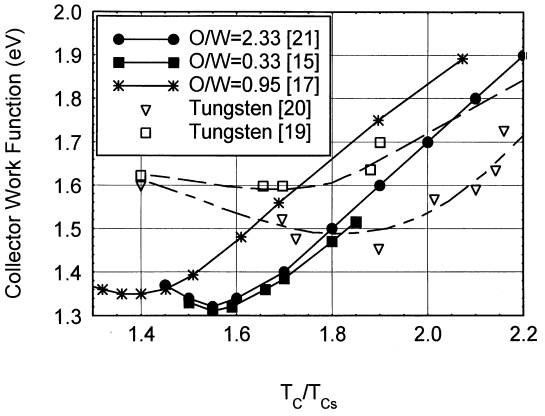

Fig. 2. Collector work function data.

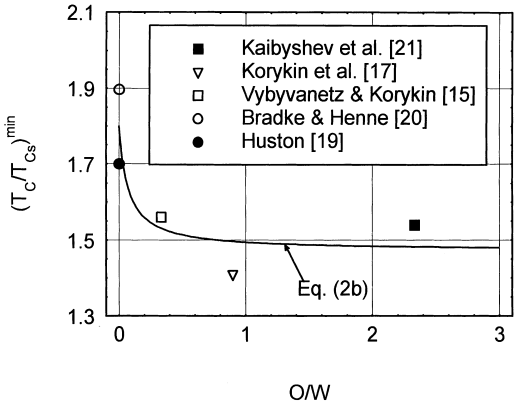

Fig. 4. (T_C/T_{Cs}) corresponding to the minimum work function of tungsten oxides.

2.33, for a tungsten oxide layer typical of that present in a TFE after outgasing [21]. As Fig. 2 shows, the lowest cesiated work functions of ~1.3 eV for tungsten oxides with O/W ratios of 0.33 and 2.33, compared to 1.5–1.6 for polycrystalline tungsten, are achieved at a lower cesium pressure (or higher T_C/T_{Cs}).

The data in Fig. 2 were used to develop two empirical correlations (Figs. 3 and 4) for predicting the minimum oxygenated–cesiated collector work function, φ_C^{min}, and the corresponding values of T_C/T_{Cs} as

$$\varphi_C^{min}(\text{eV}) = 1.288 + 0.02945(0.127556 + (\text{O/W}))^{-1}, \quad (2a)$$

$$(T_C/T_{Cs})^{min} = 1.47718 + 0.0238(0.07298 + (\text{O/W}))^{-1}. \quad (2b)$$

As Figs. 3 and 4 show, these correlations are within 0.12 eV and 0.1 of the data for the minimum collector work function and the corresponding value of T_C/T_{Cs}, respectively.

In order to obtain the collector work function for a given O/W ratio, the curve in Fig. 2 that corresponds to O/W = 0.33 was shifted in such a way that the location and the value of its minimum is determined according to Eqs. (2a) and (2b). In addition to the oxygenated–cesiated work function of the tungsten oxides deposits on the collector surface, the effective emissivity of the electrodes was determined. The methodology used to determine the effective emissivity of the electrodes is outlined in the next section.

2.3. Effective emissivity

Tungsten oxides deposits onto the collector surface increase its thermal emissivity, beyond that of pure tungsten or molybdenum [15]. Lepage and Mezin [22] have correlated the measured thermal emissivities of tungsten oxide surfaces. The ratio of the measured emissivities of oxidized (ε_C) and non-oxidized tungsten surfaces (ε_W) is plotted in Fig. 5 versus the oxygen content in the oxide layer, at different surface temperatures. At temperatures below 900 K, the emissivity of the tungsten oxides was independent of temperature and approximately equal

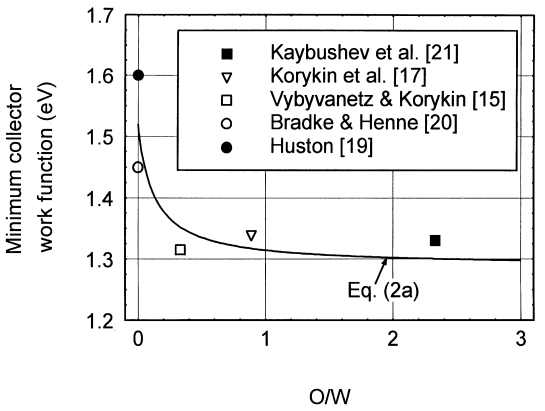

Fig. 3. Minimum collector work function correlation.

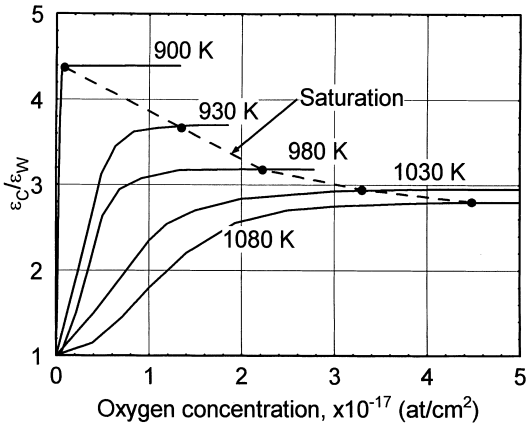

Fig. 5. Measured emissivity of oxidized tungsten [22].

at 900 K [22]. At 900 K, the emissivity reached saturation at an oxygen concentration on the collector surface of about 6×10^{15} at./cm^2, which is equivalent to a tungsten oxide (WO_3) layer that is 5×10^{-4} μm thick [22]. This thickness is much smaller than that of the deposits that could form during a nominal TFE outgasing ($\sim 6 \times 10^{-2}$ μm) [15]. Because the tungsten oxide type at saturation is WO_3 (O/W = 3), for oxide deposits in which O/W is less than 3, the corresponding oxygen concentration can be given as

$$n_O = n_O^{sat}(O/W)/3. \quad (3)$$

In the present analysis, the O/W ratio was calculated by the emitter material transport model [8]. For given oxygen concentration and collector temperature, Fig. 4 was used to calculate $\varepsilon_C/\varepsilon_W$ ratio by interpolation. For the collector temperatures below 900 K, $(\varepsilon_C/\varepsilon_W)$ was taken equal to that at 900 K (Fig. 5). Then, the effective emissivity of the TFE electrodes was calculated as

$$\varepsilon^{eff} = \left[\frac{1}{\varepsilon_W}\left(1 + \frac{1}{(\varepsilon_C/\varepsilon_W)}\right) - 1\right]^{-1}, \quad (4)$$

where ε_W is the emissivity of pure tungsten [23].

The calculated effective emissivities in a TFE having a tungsten emitter and a collector covered with tungsten oxides are compared in Fig. 6, with reported data of TOPAZ-II type TFEs at the beginning of life [10] and of the TFEs of the TOPAZ-II Ya-21u unit [24], which were contaminated due to air excursion into the interelectrode gap. At an emitter temperature of 2000 K, the effective emissivity for a tungsten emitter and pure molybdenum collector is less than 0.1, while the measured emissivity for the as manufactured TFEs is about 0.17. Such a difference between theoretical and actual effective emissivities of the electrodes was attributed to the presence of tungsten oxides deposits onto the collector surface, which could have formed during the TFE outgasing [2,15]. As Fig. 6 shows, the O/W ratio in the deposits on the collector surface of a TOPAZ-II type TFE after outgasing could have been about 0.66, and close to 3.0 for the Ya-21u unit TFEs.

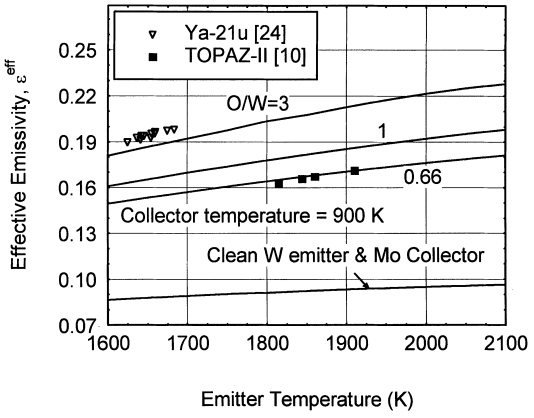

Fig. 6. Effective emissivity of a TOPAZ-II type TFE.

3. Analysis

In the present analysis of a fission heated single-cell TOPAZ-II type TFE, the emitter is made of monocrystalline molybdenum alloyed with 3% niobium, coated with a 0.1 mm thick monocrystalline tungsten layer having a preferred crystallographic orientation alternating azimuthally between ⟨1 1 0⟩ and ⟨1 1 2⟩. The collector assembly consists of a collector tube, a 0.15 mm thick Al_2O_3 insulation on the outer surface, and a He filled gap (0.05 mm thick) separating the Al_2O_3 insulation from the stainless-steel wall (0.35 mm thick) of the coolant channel. In order to maintain uniform interelectrode gap along the active length of the TFE (375 mm), the TFE has six Nb alloy inserts, each having nine grooves to accommodate scandium oxide (Sc_2O_3) spacers. These spacers maintain a uniform gap size between the electrodes along the active length of the TFE. Details on the TOPAZ-II type TFE design can be found elsewhere [9,10].

The effects of O/Cs atom ratio on the TFE performance and on the emitter material loss rate at a thermal power input to the emitter, P_{th}, of 3500 W are investigated. The axial distribution of the fission thermal input to the emitter was a chopped cosine [9]. The cesium pressure, P_{Cs}, the inlet temperature and mass flow rate of NaK liquid coolant are taken equal to 133 Pa, 773 K and 0.04 kg/s, respectively. The initial composition of the collector surface will depend on the TFE conditions before outgasing and on the outgasing scenario. For consistency, however, the present analysis assumes that the composition of the collector surface is solely determined by the emitter material deposits. Thus, in the case where there is no or little oxygen present in the interelectrode gap, no tungsten oxides will be deposited onto the collector and its surface composition is taken as tungsten. This condition, however, might not occur in practice because at the beginning-of-life, the TFE collector would be already covered with tungsten oxides, due to the presence of oxygen contaminants in the interelectrode gap during outgasing.

3.1. Axial variation of TFE operation parameters

The calculated axial distributions of the TFE parameters as functions of the load voltage at O/Cs = 10^{-8} are shown in Fig. 7. The emitter temperature decreased from its maximum at the TFE mid-plane ($z = 0.1875$ m) toward both ends. This 'bell' shaped axial temperature distribution differs from the chopped cosine distribution of the thermal power input, because of the

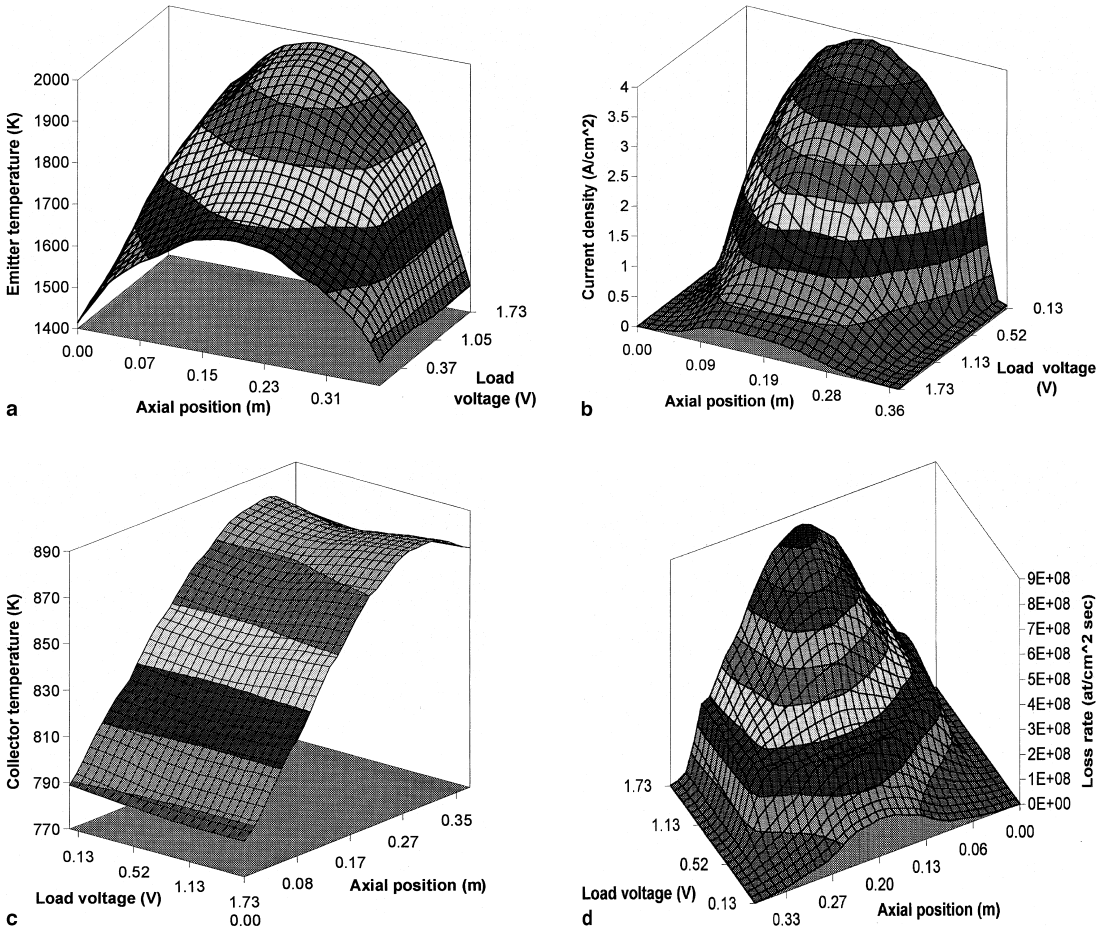

Fig. 7. Calculated axial variation of TFE conditions at $P_{th} = 3500$ W, $P_{Cs} = 133$ Pa and O/Cs $= 10^{-8}$: (a) Emitter temperature; (b) current density; (c) collector temperature; (d) tungsten loss rate.

thermal loss due to axial heat conduction through the top and the bottom ends of the TFE [9]. The emitter temperature decreased, but its axial distribution became more uniform as the load voltage decreased, increasing the current density (Fig. 7(b)). The heat transfer rate to the collector, which is the difference between the input thermal power to the emitter minus the thermal losses and the TFE output electric power, depends on the load voltage. Both the collector temperature (Fig. 7(c)) and its oxygenated–cesiated work function depend on the load voltage. As Fig. 7(c) shows, the lowest collector temperature and, hence, its minimum oxygenated–cesiated work function occurred at a load voltage of 0.7 V, which is the optimum load voltage for the conditions considered in the present analysis (Fig. 7).

The calculated tungsten loss rate from the emitter surface along the TFE for O/Cs $= 10^{-8}$ (Fig. 7(d)) varied also with the load voltage and axial position, commensurate with the axial emitter temperature distribution. The tungsten loss rate was highly non-uniform along the TFE, having a peak-to-average ratio of about 2. The tungsten loss rate decreased as the load voltage decreased (Fig. 7(d)), since a lower load voltage corresponds to a lower emitter temperature (Fig. 7(a)). However, in the range from 0.37 to 0.55 V, the tungsten loss rate is almost constant along the central portion of the TFE ($z = 0.06$ to 0.32 m) (Fig. 7(d)), where the emitter temperatures varied within a narrow range (1720–1780 K).

3.2. Effect of oxygen on TFE performance and emitter tungsten loss rate

The calculated static volt–ampere and volt–watt characteristics of the single-cell TFE for O/Cs ratios from 0 to 10^{-6} are shown in Fig. 8(a) and (b), respectively. Increasing the O/Cs ratio up to 10^{-8}, increased the TFE electric power output in the ignited mode (load voltage <1 V). This is because the load voltage (and the load electric power) increased as tungsten oxides

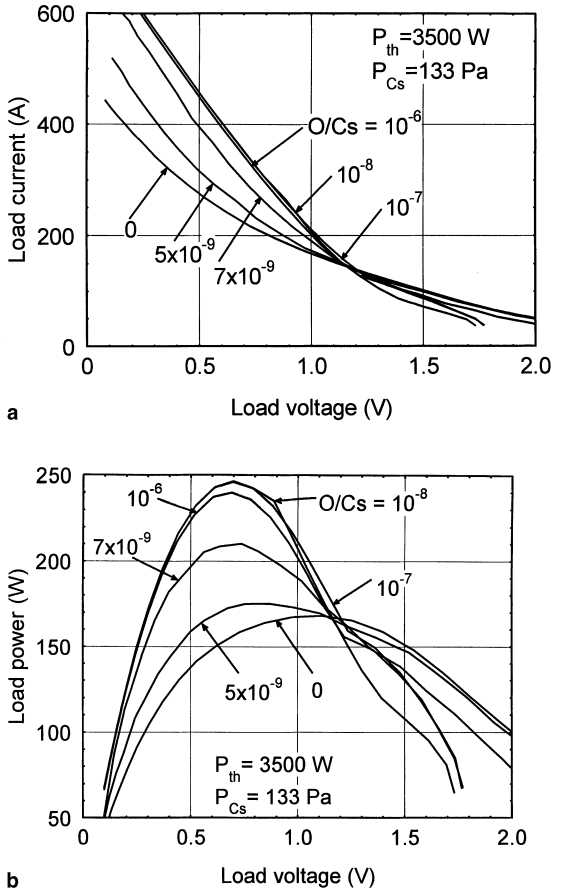

Fig. 8. (a) Calculated volt–ampere characteristics of a TOPAZ-II type TFE in presence of oxygen. (b) Static volt–watt characteristics of a TOPAZ-II type TFE in presence of oxygen.

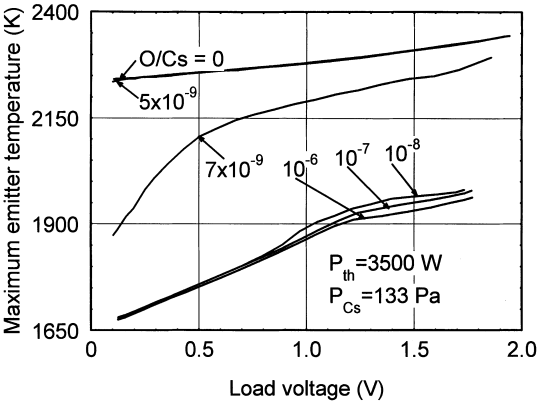

Fig. 9. Calculated maximum emitter temperature.

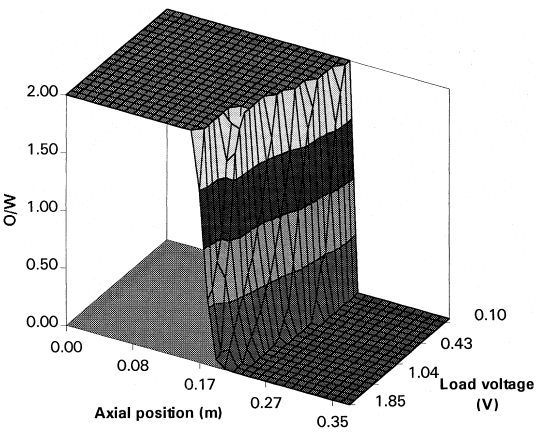

Fig. 10. Calculated chemical composition of deposits on collector at O/Cs = 7×10^{-9}, $P_{th} = 3500$ W and $P_{Cs} = 133$ Pa.

with a lower cesiated work functions (Fig. 2) deposited onto the collector surface. The presence of tungsten oxides onto the collector surface also increased the TFE effective emissivity (Fig. 6), resulting in a lower emitter temperature (Fig. 9) and higher emitter coverage with cesium, thus increasing the emission current. Conversely, in the unignited mode (load voltage >1 V) higher O/Cs ratio and lower emitter temperature resulted in a lower TFE electric performance (Fig. 9).

Fig. 9 delineates the effect of changing the O/Cs ratio in the interelectrode gap on the maximum emitter temperature and on the composition of the deposits. When there was no or little oxygen present (O/Cs = 5×10^{-9}), the maximum emitter temperature was high due to the low effective emissivity of the TFE electrodes (Fig. 6). At O/Cs = 7×10^{-9}, however, the collector surface was partially covered with WO_2 (Fig. 9), which has higher emissivity, thus lowering the emitter temperature. When O/Cs ratio in the interelectrode gap increased to O/Cs > 10^{-8}, the collector was completely covered with WO_2 (O/W = 2). As a result, the maximum emitter temperature was significantly lower, but weakly dependent on the O/Cs ratio. For any O/Cs ratio, the maximum emitter temperature increased as the load voltage decreased due to change in the emitter electron cooling.

Fig. 10 shows the calculated composition of the deposits along the collector as a function of the load voltage for a O/Cs ratio of 7×10^{-9}. The composition of the oxide deposits changed from WO_2 (O/W = 2) to W, as the collector temperature increased axially from the inlet to the exit of the TFE. Changing the load voltage insignificantly affected the composition of the deposits (Fig. 10), because the associated change in the collector temperature was small. For the volt–ampere characteristics corresponding to a O/Cs ratio of 5×10^{-9} and zero (Fig. 8), only W was deposited on the collector. When the O/Cs ratio increased to 10^{-6}, the collector was completely covered with WO_3. The high effective emissivity of WO_3 (Fig. 6), lowered the emitter temperature below

its optimum value for 133 Pa cesium pressure, reducing the load current (Fig. 8).

The calculated maximum tungsten loss rates (which correspond to the maximum emitter temperatures in the TFE) (Fig. 7(a)) are shown in Fig. 11, as functions of the load voltage and O/Cs ratio in the interelectrode gap. The maximum loss rate of the emitter tungsten increased as the load voltage and, hence, the emitter temperature increased (Fig. 9). With little or no oxygen present in the interelectrode gap, the tungsten loss rate from the emitter surface (Fig. 11) was directly proportional to the emitter temperature (Fig. 9). At $O/Cs = 10^{-8}$, the tungsten loss rate was minimum, because the collector was completely covered with WO_2, increasing the effective emissivity and, hence, resulting in a lower emitter temperature (Fig. 8). At the same time, however, the oxygen partial pressure in the interelectrode gap was insufficient to cause significant tungsten loss in the form of volatile oxides. As the amount of oxygen in the interelectrode gap increased, the tungsten loss rate at higher load voltages rose by an order of magnitude (Fig. 11). At such high oxygen partial pressures, the rate of emitter tungsten loss in the form of volatile tungsten oxides continued to increase as the oxygen partial pressure (or O/Cs ratio) increased, while the emitter temperature decreased only slightly (Fig. 9).

3.3. Effect of cesium pressure

The effect of cesium pressure on the TFE electric power output in the presence of oxygen in the interelectrode gap is delineated in Fig. 12. The maximum TFE electric power output P_{max}^{load}, corresponds to the optimum load voltage which depends on both O/Cs ratio in the interelectrode gap and P_{Cs} (Fig. 8(a)). When the oxygen partial pressure was small, there were no tungsten oxides deposited onto the collector surface and the emitter temperature was high (Fig. 9), resulting in a weak dependence of the TFE electric power output on O/Cs ratio. At these conditions, the TFE electric power output, however, was strongly dependent on P_{Cs} peaking at 400 Pa (Fig. 13). Further increase in the partial pressure of oxygen in the interelectrode gap (up to $O/Cs > 2 \times 10^{-9}$ for $P_{Cs} = 100$ Pa and $O/Cs > 2 \times 10^{-8}$ for $P_{Cs} = 532$ Pa) caused tungsten oxides to deposit onto the collector surface. At low P_{Cs} (<200 Pa) the deposition of tungsten oxides onto the collector surface increased P_{max}^{load} due to the lower oxygenated–cesiated emitter and collector work functions. At the optimum P_{Cs} or higher (400 and 532 Pa), increasing O/Cs up to 4×10^{-8} increased O/W ratio in the deposits, reducing the TFE electric power output due a to further reduction of the emitter temperature. As O/Cs ratio increased further, P_{max}^{load} decreased at all values of P_{Cs} (Fig. 12).

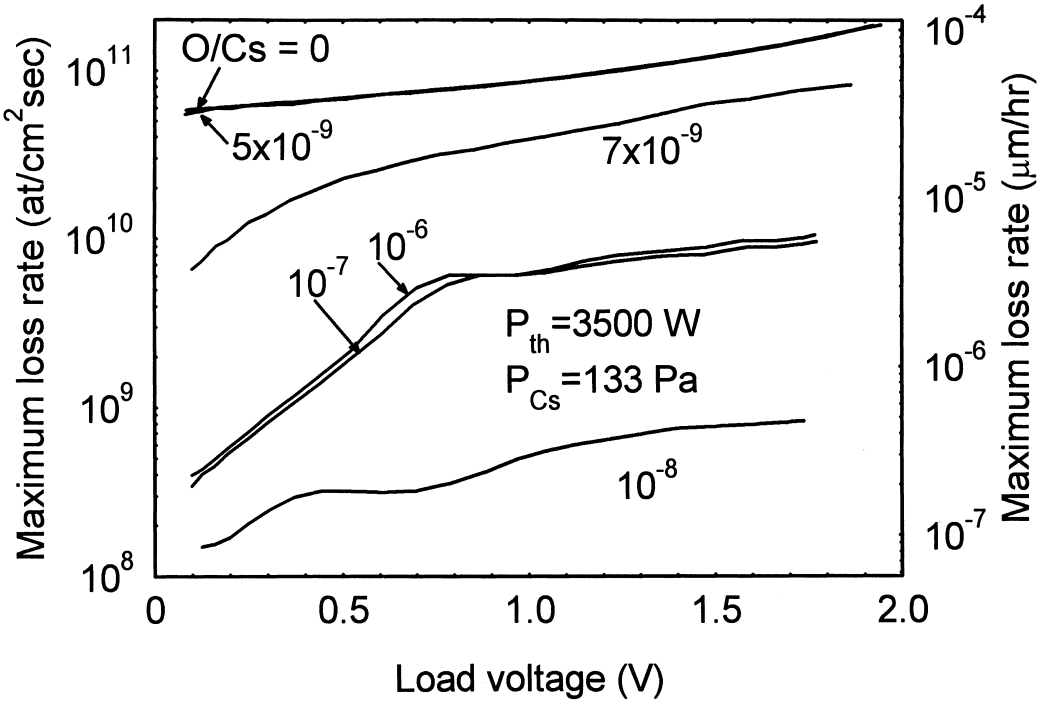

Fig. 11. Calculated maximum tungsten loss rate.

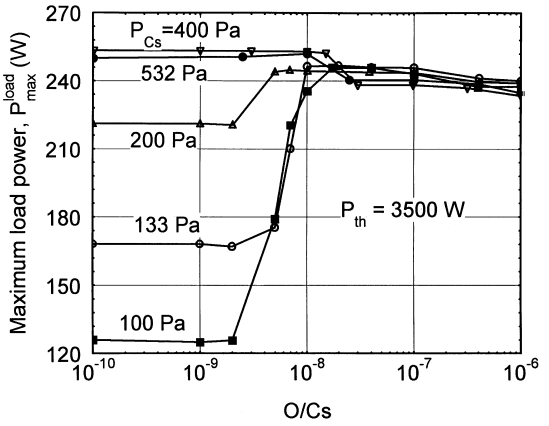

Fig. 12. Effect of O/Cs ratio on TFE output power.

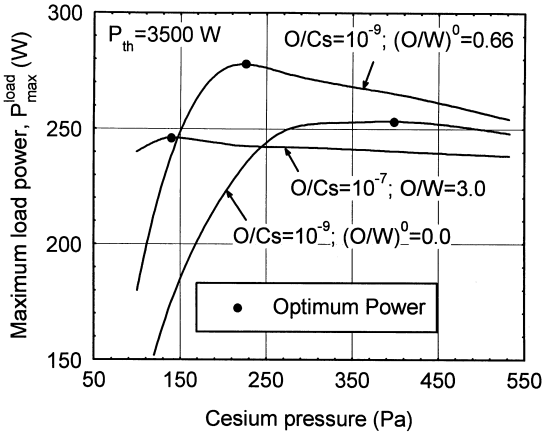

Fig. 13. Effect of cesium pressure on TFE output power.

Fig. 13 compares P_{max}^{load} for $O/Cs = 10^{-9}$ and 10^{-7} as a function of P_{Cs}. At a low partial pressure of oxygen ($O/Cs = 10^{-9}$), the TFE load electric power was always higher when $(O/W)^0 = 0.66$ (Fig. 6), compared to a pure tungsten collector ($(O/W)^0 = 0.0$). Such a high maximum electric load power was caused by the low cesiated work function of the tungsten oxides deposits (Fig. 2). Because these oxides also have higher emissivity (Fig. 6), the emitter temperature and, respectively, the optimum P_{Cs} were lower than for a pure tungsten collector (Fig. 13).

The results also show that when $O/Cs = 10^{-7}$, the collector was covered with WO_3 oxides ($O/W = 3.0$). The high thermal emissivity of WO_3 (Fig. 6) was responsible for the low TFE maximum load power (Fig. 13). The cesiated emitter work function and, respectively, P_{max}^{load} were weakly dependent on P_{Cs} at $O/Cs = 10^{-7}$ (Fig. 13). The optimum P_{Cs} at these conditions was only 146 Pa, compared to 226 and 400 Pa at $O/Cs = 10^{-9}$, and $(O/W)^0 = 0.66$ and $(O/W)^0 = 0.0$, respectively. The results in Fig. 13 showed that the presence of oxygen in the interelectrode gap at $O/Cs = 10^{-7}$ increased P_{max}^{load} only at low P_{Cs} (<146 Pa). The presence of tungsten oxides with $O/W = 0.66$ on the collector surface resulted, however, in the best TFE performance at all values of P_{Cs} > 146 Pa. This is consistent with the results of the investigations of the effects of oxygen on the performance of a planar TIC having a uniformly heated emitter shown in Fig. 14 [25]. The input thermal flux of 20 W/cm^2 in Fig. 14 is close to the average value in the single-cell TFE when operated at $P_{th} = 3500$ W (Fig. 13). As Fig. 14 shows, the optimum P_{Cs} values for the TFE and the planar converter were close at all values of O/Cs and $(O/W)^0$. The best converter performance corresponds to the low partial pressure of oxygen in the interelectrode gap ($O/Cs = 10^{-9}$), when the collector was initially covered with the tungsten oxides having $(O/W)^0 = 0.66$. Contrary to the TFE, however, the peak power density of the planar converter at $O/Cs = 10^{-7}$ was slightly higher (by 0.1 W/cm^2) than at $O/Cs = 10^{-9}$ for a pure tungsten collector. This is due to the fact that the electrodes of a planar TIC are isothermal [25], while the temperature of the electrodes and the current density along the TFE electrodes are axially non-uniform (Fig. 7(a)–(c)).

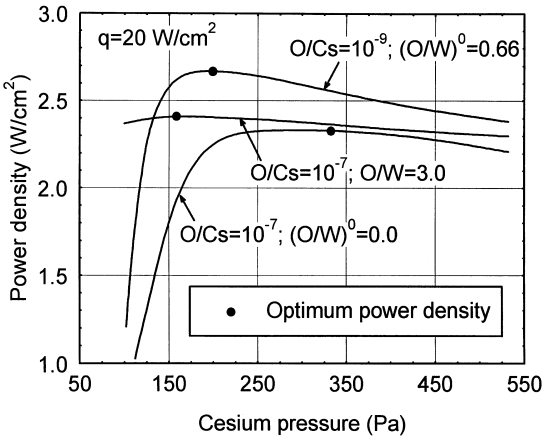

Fig. 14. Effect of cesium pressure on power density of a planar thermionic converter [25].

4. Summary and conclusions

An integrated model of a single-cell TFE has been developed which calculates not only the emitter material (tungsten) loss rate in the presence of oxygen in the interelectrode gap, but also predicts the effects of the tungsten oxides deposits on the collector surface on the TFE performance. The methodologies used for determining the effective emissivity and the oxygenated–cesiated work functions of the electrodes are described. The

results for a fission heated, single-cell, TOPAZ-II type TFE, operating at $P_{th} = 3500$ W and $P_{Cs} = 133$ Pa, showed that a small partial pressure of oxygen (O/Cs $\approx 10^{-8}$) in the interelectrode gap increases the electric power output beyond that of a TFE having a pure tungsten collector. Such improvement in performance is caused by the decrease of the oxygenated–cesiated work functions of both the emitter and collector. At a higher oxygen pressure in the interelectrode gap (O/Cs $= 10^{-6}$), the collector would be completely covered with WO_3, which increases the effective emissivity of the electrodes and causes both the emitter temperature and the load current in the ignited mode to decrease. This decrease in the TFE electric power output at a high partial pressure of oxygen is independent of P_{Cs}.

The results also showed that at O/Cs $= 10^{-8}$, the emitter tungsten loss rate is minimum ($\sim 9 \times 10^{-8}$–5×10^{-7} μm/h), due to the low emitter temperature and its low coverage with oxygen. As the O/Cs ratio increased from 10^{-8} to 10^{-6}, the tungsten loss rate, at a load voltage of 1 V, rose by more than an order of magnitude (from 3×10^{-7} to 6×10^{-6} μm/h), while the emitter temperature decreased only slightly. The tungsten loss rate is highly non-uniform along the TFE owing to the non-uniform axial emitter temperature distribution. The tungsten loss rate is highest at the TFE mid-plane, where the emitter temperature is maximum, and decreases as the load voltage decreases, because of the associated reduction in the emitter temperature.

Analysis of the effects of cesium pressure and the collector surface composition showed that the best TFE performance is achieved for a collector surface composition typical of that in a TFE after outgasing ($(O/W)^0 = 0.66$) and at a small partial pressure of oxygen (O/Cs $= 10^{-9}$). As O/Cs ratio increases to 10^{-7}, the TFE electric power output at both the optimum load voltage and the optimum cesium pressure decreases by approximately 30 W.

The implications on the design of oxygenated TICs and TFEs can be summarized as follows:

- TFE power and conversion efficiency corresponding to the optimum cesium pressure and load voltage can be significantly enhanced by the introduction of a tracer amount of oxygen (partial pressure $\leqslant 10^{-6}$ Pa) into the interelectrode gap, which is consistent with recent experimental results [4].
- Because of the non-uniform TFE axial emitter temperature distribution, the performance gain due to the introduction of oxygen into the interelectrode gap of a TFE is less than that expected for a planar isothermal TIC [25].
- A partial oxygen pressure that is higher than optimum ($>10^{-6}$ Pa) would accelerate the emitter material loss and change the collector surface properties, particularly, the thermal emissivity of the electrodes, which, in turn, lowers the TFE performance.
- Besides changing the collector surface properties, the high oxygen pressure and the induced high emitter material loss rate could shorten TFE operation lifetime due to the buildup of the emitter material oxides onto the surfaces of the collector, spacers, and insulators.

Acknowledgements

This research was partially sponsored by the Defense Special Weapons Agency through the New Mexico Engineering Research Institute under contract DNA001-96-C-00291 to the University of New Mexico's Institute for Space and Nuclear Power Studies.

References

[1] J. McVey, personal communications, Albuquerque, NM, 1991.
[2] V.A. Korykin, V.P. Obrezumov, V.I. Vybyvanets, in: Proc. of the 24th IECEC, Institute of Electrical and Electronics Engineers, vol. 2, New York, 1989, p. 1161.
[3] J.-L. Denisot, Electron emission experimental study of a (1 0 0) tungsten single crystal covered with cesium and oxygen, Report CEA-R-4508, Commissariat a l'Energie Atomique, France, 1973.
[4] C.B. Geller, C.S. Murray, D.R. Riley, J.-L. Desplat, L.K. Hansen, G.L. Hatch, J.B. McVey, N.S. Rasor, Final Report of the High Efficiency Thermionic (HET-IV) and Converter Advancement (CAP) Programs, Report No. WAPD-T-3108, Westinghouse Bettis, Pittsburgh, PA, 1995.
[5] P. Rouklove, in: Proc. Second Int. Conf. on Thermionic Electric Power Generation, Euratom Center for Information and Documentation, Stresa, Italy, 1968, p. 61.
[6] D. Lieb, D. Goodale, T. Briere, C. Balestre, in: Proc. 12th IECEC, vol. 3, American Nuclear Society, La Granda Park, Illinois, 1977, p. 1555.
[7] M. Clemot, B. Gayte, R. Lebourg, Post test examinations of a long life thermionic converter, in: Proc. Thermionic Conversion Specialist Conference, Miami, Florida, 1970, pp. 556–561.
[8] D.V. Paramonov, M.S. El-Genk, in: M.S. El-Genk (Ed.), Proc. 13th Symp. on Space Nuclear Power and Propulsion, AIP Proceedings #361, American Institute of Physics, vol. 3, New York, 1996, p. 1137.
[9] M.S. El-Genk, H. Xue, J. Nucl. Tech. 108 (1994) 112.
[10] Y.V. Nikolaev, Y.G. Degaltsev, B.S. Stepennov, V.P. Nikitin et al., Thermionic Fuel Elements of Power Plant TOPAZ-II, JV INERTEK, Moscow, Russia, 1991.
[11] N.S. Rasor, in: Proc. 1970 Thermionic Conversion Specialist Conference, Institute of Electrical and Electronics Engineers, New York, 1970, p. 181.
[12] W. Engeimaier, R.E. Sticney, Surf. Sci. 11 (1968) 370.
[13] N.S. Rasor, C. Warner, J. Appl. Phys. 35 (1964) 2589.
[14] V.A. Zherebtsov, M.A. Lebedev, A.A. Lukyanov, A.A. Sobolev, TEC mode effect on the emitter–collector mass-transfer, Second International Conference Nuclear

Power in Space, USSR Ministry of Atomic Energy, Sykhumi, USSR, 1991, pp. 109–115.
[15] V.I. Vybyvanetz, V.A. Korykin, Mass transport in interelectrode gap and its impact upon electrode properties and TFE characteristics, JV INERTEK, Report SP-1145/5474-3.1.16, Moscow, Russia, 1993.
[16] W. Wagner, J. Ewers, W. Pentermann, J. Chem. Thermodyn. 8 (1976) 1049.
[17] V.A. Korykin, V.P. Obrezumov, V.I. Vybuvanetz, Yu.V. Nikolaev, Processes in interelectrode gap, on electrodes and TFE lifetime, in: Proceedings of the Nuclear Power in Space Conference Sukhumi, USSR Ministry of Atomic Energy, Sukhumi, 1991, pp. 100–110.
[18] M. Bradke, I. Halder, The work function of oxygen covered surfaces in barium and cesium vapor, in: Proceedings of the Thermionic Conversion Specialists Meeting, Eindhoven University of Technology, Eindhoven, Netherlands, 1975, pp. 31–36.
[19] J.M. Huston, H.F. Webster, Adv. in Electron and Electron Phys. 17 (1962) 125.
[20] M. Bradke, R. Henne, in: Proc. 10th Intersociety Energy Conversion Engineering Conf. Society of Automotive Engineering, 1975, p. 382.
[21] V.Z. Kaibyshev, V.A. Korykin, V.P. Obrezumov, Atomn. Ener. 69 (1990) 196.
[22] J. Lepage, A. Mezin, Vacuum 43 (1992) 1185.
[23] G.G. Gubareff, J.E. Jansen, R.H. Torborg, Thermal radiation properties survey, Honeywell Research Center, Minneapolis-Honeywell Regulator Company, Minneapolis, Minnesota, 1960.
[24] D.V. Paramonov, M.S. El-Genk, in: M.S. El-Genk (Ed.), Proceedings 13th Symposium on Space Nuclear Power and Propulsion, AIP Proceedings #361, vol. 3, American Institute of Physics, New York, 1996, p. 1267.
[25] D.V. Paramonov, M.S. El-Genk, Energy Conv. Management 39 (5) (1998) 375.